

# A case of coronary arterio-venous fistula: the role of cardiac computed tomography

Ernesto Forte, Teresa Infante, Dario Baldi, Marco Salvatore, Filippo Cademartiri, Carlo Cavaliere

IRCCS SDN, Naples, Italy

Correspondence to: Ernesto Forte. IRCCS SDN, via E. Gianturco 113, 80143 Naples, Italy. Email: eforte@sdn-napoli.it.

Submitted May 15, 2018. Accepted for publication Aug 01, 2018.

doi: 10.21037/jtd.2018.08.69

View this article at: <http://dx.doi.org/10.21037/jtd.2018.08.69>

## Introduction

Coronary artery fistulas (CAFs) are often incidental findings in patients undergoing conventional coronary angiography (CAG). CAFs represent a congenital or acquired abnormal vascular communication of coronary arteries with cardiac chambers or any segment of the systemic or pulmonary circulation bypassing capillaries within myocardium (1). Patient may present with non-specific symptoms such as dyspnea or asymptomatic (2). The origin and the drainage site are important for patient management and eventually for clinical treatment. Unlike CAG, cardiac computed tomography (CCT) gives a comprehensive overview of coronary vessel course, diameter, and wall, not to mention the relationship with all the surrounding structures (3); ejection fraction and ventricular volumes can be quantified together with Qp/Qs ratio, kinetic alterations and perfusion analysis.

## Case presentation

A 50-year-old asymptomatic man was referred to our institution with suspicion of aortic dissection at the echography. Cardiovascular risk factors included smoking, dyslipidemia and hypertension under treatment with a dietary supplement and  $\beta$ -blocker, respectively. He underwent a CCT with a 3<sup>rd</sup> generation dual source multidetector computed tomography (CT) scanner (Somatom Force, Siemens Healthcare AG, Erlangen, Germany). A prospectively ECG-triggered high pitch spiral acquisition (FLASH) non-contrast CT was performed for calcium score evaluation. Afterwards we performed an angiographic CT scan with retrospective ECG gating; the scan was performed with automated attenuation-based

anatomical tube current modulation (CARE Dose4D, Siemens) and tube voltage was selected by the use of an automated attenuation based tube voltage selection functionality (CARE kV, Siemens). For the angiographic scan the patient received intravenously 70 mL of iodinated contrast agent (iomeprol 400 mgI/mL, Iomeron 400, Bracco, Italy) at 5.5 mL/s followed by 50 mL of saline flush at the same flow.

Data were reconstructed with a dedicated 3<sup>rd</sup> generation advanced modeled iterative reconstruction (ADMIRE, Siemens) with strength level of 3 using medium sharp convolution kernels (Bv36 and Bv40), at best diastolic and best systolic phases (the absolute delay expressed in ms from the R wave was used) with a section thickness of 0.75 mm and an increment of 0.4 mm; pixel matrix size 512×512. In addition, a multiphasic dataset ranging from 0% to 95% of the cardiac R-R cycle was also reconstructed with a section thickness of 1.5 mm and an increment of 1 mm, pixel matrix size 256×256, convolution kernel Qr32, iteration ADMIRE 4. Images were analyzed on an offline dedicated workstation (syngo.via VB10B, Siemens) where MIP, c-MPR and 3D volume rendering images were generated. The heart rate during scan was 53 bpm. Calcium score was 2,356 according to Agatston method (99<sup>th</sup> percentile based on age and gender).

The RCA originated from the right aortic sinus and appeared diffusely dilated with a tubular pattern (maximum diameter 12 mm), tortuous and atheromatous with no significant obstructive stenosis, and terminated at the crux cordis into a large fistulous plexus (maximum diameter 45 mm) connected to coronary sinus (*Figure 1*). The fistula presented a knot-like shape involving both the coronary artery and the great cardiac vein (*Figures 2,3*). At rest perfusion analysis

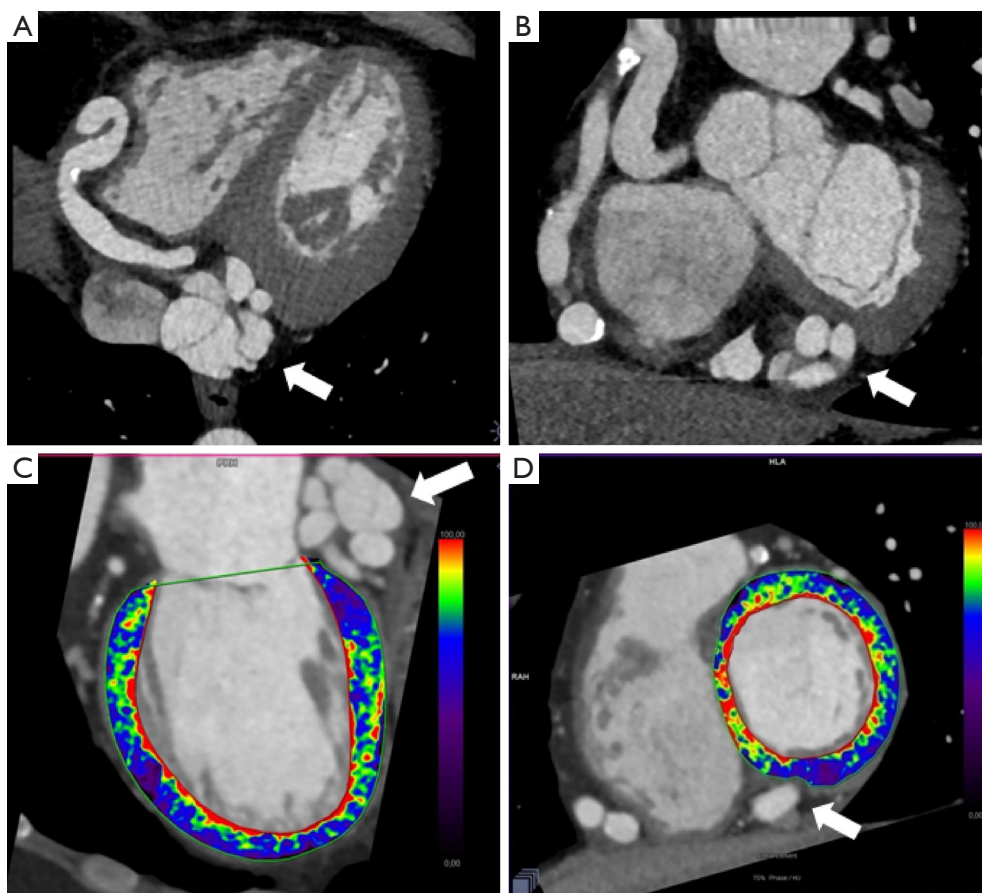


**Figure 1** Axial and basal short axis CT images representing the coronary arterio-venous fistula (white arrow). The vessel carries out tortuous kinkings before reaching the crux cordis (A,B); (C,D) perfusion maps: long axis and short axis views representing the inferior defects near fistula and the anterior defects in myocardium supplemented by LAD. LAD, left anterior descending artery.



**Figure 2** The course of the arterio-venous fistula is reproduced ranging from the acute margin to the obtuse margin (4).

Available online: <http://www.asvide.com/article/view/27403>

revealed a segmental transmural defect on the basal inferior myocardial wall adjacent to the coronary fistula ( $37.21 \pm 3.04$  vs.  $85 \pm 5$  HU in remote septal myocardium) (Figure 1C,D). Moreover, a mixed eccentric plaque causing a significant stenosis was detected on the middle left anterior descending artery (LAD) with a significant hypoperfusion on the anterior myocardial wall ( $40 \pm 3$  HU). Despite the preserved ejection fraction (70%) and global systolic function, both the left and the right ventricle were dilated (VTD =  $104.66$  and  $117.6$  mL/m<sup>2</sup>); the Qp/Qs = 1.1, calculated according to the method proposed by Osawa *et al.* (5), revealed a non-significant left to right shunt. There was neither myocardial wall alteration nor evidence of aortic dissection.

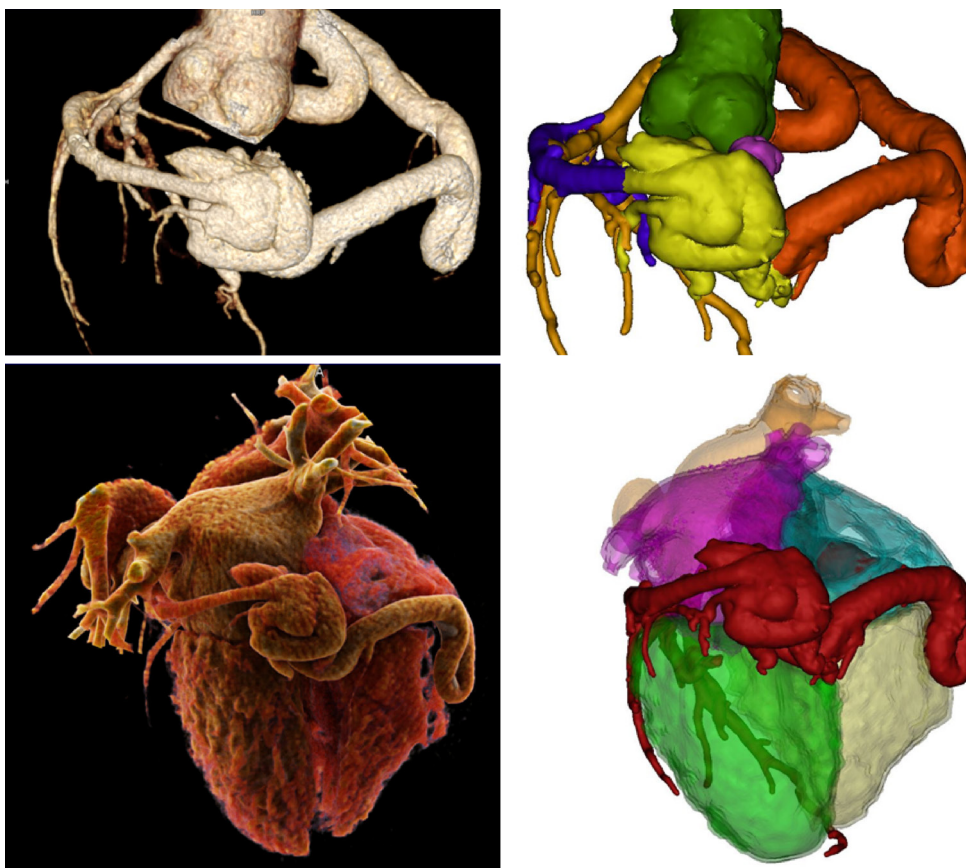


**Figure 3** Upper panels: vascular tree rendering (ascending aorta in green, right coronary artery in orange, left coronary artery in brown, great cardiac vein in blue, fistula in yellow, coronary sinus in violet). Lower panels: 3D volume rendering (left ventricle in green, right ventricle in grey, vascular tree in red, left atrium in violet, right atrium in blue, pulmonary trunk in orange).

## Discussion

CAFs consist in an abnormal communication between the coronary arteries and other vascular structures or cardiac chambers bypassing the myocardial capillary bed (6). CAFs can be classified according to their origin, drainage site or complexity and have a prevalence of 0.002% in the general population increasing to 0.05–0.25% in patients undergoing CAG (7). At CCT, the origin site is the right coronary artery in 50–55% of patients, the LAD artery in 35–42% of patients and both the RCA and LAD in 5% of patients; the origin from the left circumflex coronary artery is uncommon (8). According to the drainage site, CAFs can be classified in to “coronary cameral fistula” where a coronary artery drains in to a cardiac chamber and “coronary arterio-venous fistula” indicating a communication between a coronary artery and a low-pressure vein or vascular cavity such as pulmonary artery, coronary sinus, superior

and inferior vena cava, bronchial vessels and extracardiac veins (1). At CCT, the most common drainage site is the venous system (90%), the coronary sinus is found in 7% of patients (8), the bronchial artery in 0.61% of patients while the coronary-to-pulmonary artery fistulas account for 15–30% of all CAFs and in the 89% of cases drain in to the pulmonary trunk (1).

Even if most patients are asymptomatic, in some cases they present with typical signs (continuous heart murmur, right ventricular enlargement, cardiac dysfunction, endocarditis and arrhythmias) and symptoms (dyspnea, orthopnea, fatigue and chest pain) (6). Congenital CAFs are essentially due to persistence of sinusoids, which in normal heart nourish the trabecular myocardium but, at approximately 32 days of gestation, after myocardial compaction, are replaced by arteries, veins and capillaries (9). From a pathophysiological point of view, CAFs change course to myocardial blood flow

causing its reduction downstream of the fistula with possible consequent ischemia to the supplied myocardial territories. Subsequently, the fistulous coronary artery can undergo a compensatory mechanism driven by the pressure gradient existing between the two communicating structures and leading to coronary enlargement or notable tortuous course, with several possible complications such as aneurysm development, atherosclerotic deposition, and even rupture in a few cases (2,10).

Medical imaging is fundamental to assess the location and size of the fistulas and allows the differential diagnosis of CAFs with other diseases presenting with dilated or tortuous coronaries as anomalous left coronary artery arising from the pulmonary artery (ALCAPA), Kawasaki disease, Takayasu arteritis and coronary artery ectasia related to atherosclerosis (1).

The reference standard technique has been represented by CAG (in absence of any alternative imaging technique to display coronary anatomy) by which, at the same time, both diagnosis and endovascular procedures can be performed. However, CAG is invasive, the anatomical relationships with surrounding structures are not visualized, and, even more important, the high flow of the fistula results in high flux of contrast agent with consequent decreased vessel attenuation so it can be very difficult to obtain a complete and sharp definition of the fistula itself. In the last decades, cardiac magnetic resonance (CMR) and CCT have been developed. CMR provides several tools to assess cardiac function and tissue characterization but coronary display is limited to the proximal course, mainly due to the lower CMR spatial resolution and contrast-to-noise ratio compared to CCT (1,11). Moreover, MRI of the coronary arteries is markedly limited by trigger and motion artifacts, it is time consuming and still represents a research field not being widespread in clinical practice. Despite the use of ionizing radiation, CCT is the non-invasive reference standard for the imaging of the coronary tree; the volumetric approach and high spatial resolution of CCT render quite easy to show coronary anomalies and the presence of coronary artery disease (12). The cutting edge technologies have led to both morphological and functional analysis, fast acquisition, implementation of low-dose protocols and good image quality also in patients with high heart rate.

As regards at rest perfusion analysis, even though it is able to identify resting perfusion defects associated with previous myocardial infarction and resting ischemia due to hemodynamically significant coronary stenosis, it is based only on Hounsfield unit measurements and is very prone

to artifacts so ischemic myocardium may go undetected and a vasodilator stress CT perfusion imaging is needed to definitively evaluate for ischemia (13).

In our case, CCT allowed an accurate diagnosis revealing a large fistula draining in to the coronary sinus associated to a significant obstructive coronary artery disease. The RCA appeared markedly dilated with several calcifications and multiple kinkings and the LAD presented a significant obstructive stenosis. Cardiac function analysis showed that both the right and the left ventricle were enlarged but the ejection fraction was preserved and there was no significant left-to-right shunt, even though biventricular volumes resulted increased. Moreover, perfusion analysis unmasked the abovementioned myocardial steal phenomenon.

The management of CAFs include close monitoring, generally in asymptomatic patients, and treatment by surgical ligation or percutaneous transcatheter closure with occlusion coils or umbrella devices in case of symptoms, unfavorable features or evidence of large shunt ( $Q_p/Q_s > 1.5$ ) (6). In our case, the patient was recommended to a specialist consult after which a conservative management with follow up surveillance examinations was advocated.

In conclusion, CCT is a versatile tool that allows not only coronary visualization but also functional and perfusion analysis. In our case, the coronary tree alteration has been clearly depicted and perfusion analysis, even if it should be used with caution, highlighted the myocardial steal phenomenon.

### Acknowledgements

*Funding:* This study was supported by the grants from the Italian Ministry of Health (Project Code: GR-2011-02349436).

### Footnote

*Conflicts of Interest:* The authors have no conflicts of interest to declare.

*Informed Consent:* Written informed consent was obtained from the patient for publication of this case report and any accompanying images.

### References

1. Yun G, Nam TH, Chun EJ. Coronary Artery Fistulas: Pathophysiology, Imaging Findings, and Management.

- Radiographics 2018;38:688-703.
2. Jáni L, Mester A, Hodas R, et al. Computed Tomography Assessment of Coronary Fistulas. *J Interdiscip Med* 2017;2:155-9.
  3. Forte E, Aiello M, Inglese M, et al. Coronary artery aneurysms detected by computed tomography coronary angiography. *Eur Heart J Cardiovasc Imaging* 2017;18:1229-35.
  4. Forte E, Infante T, Baldi D, et al. The course of the arterio-venous fistula is reproduced ranging from the acute margin to the obtuse margin. *Asvide* 2018;5:784. Available online: <http://www.asvide.com/article/view/27403>
  5. Osawa K, Miyoshi T, Morimitsu Y, et al. Comprehensive assessment of morphology and severity of atrial septal defects in adults by CT. *J Cardiovasc Comput Tomogr* 2015;9:354-61.
  6. Karazisi C, Eriksson P, Dellborg M. Coronary artery fistulas: case series and literature review. *Cardiology* 2017;136:93-101.
  7. Zenooz NA, Habibi R, Mammen L, et al. Coronary artery fistulas: CT findings. *Radiographics* 2009;29:781-9.
  8. Saboo SS, Juan YH, Khandelwal A, et al. MDCT of congenital coronary artery fistulas. *AJR Am J Roentgenol* 2014;203:W244-52.
  9. Koenig PR, Hijazi ZM. Congenital and pediatric coronary artery abnormalities. Waltham, MA: UpToDate, 2013.
  10. Karliova I, Fries P, Schmidt J et al. Cardiac Computed Tomography as an Imaging Modality in Coronary Anomalies. *Ann Thorac Surg* 2018;105:e15-7.
  11. Infante T, Forte E, Schiano C, et al. An integrated approach to coronary heart disease diagnosis and clinical management. *Am J Transl Res* 2017;9:3148-66.
  12. Forte E, Inglese M, Infante T, et al. Anomalous left main coronary artery detected by CT angiography. *Surg Radiol Anat* 2016;38:987-90.
  13. Singh A, Mor-Avi V, Patel AR. Update on Computed Tomography Myocardial Perfusion Imaging. *Curr Cardiovasc Imaging Rep* 2016;9:19.

**Cite this article as:** Forte E, Infante T, Baldi D, Salvatore M, Cademartiri F, Cavaliere C. A case of coronary arterio-venous fistula: the role of cardiac computed tomography. *J Thorac Dis* 2018;10(9):E699-E703. doi: 10.21037/jtd.2018.08.69